This article has been accepted for publication in a future issue of this journal, but has not been fully edited. Content may change prior to final publication. Citation information: DOI 10.1109/TVT.2016.2596789, IEEE Transactions on Vehicular Technology

A Novel Spectrum Sensing for Cognitive Radio Networks with Noise Uncertainty

Mengwei Sun, Chenglin Zhao, Su Yan, Bin Li

***Abstract*—This correspondence investigates a joint spectrum sensing scheme in cognitive radio networks with unknown and dynamic noise variance. A novel Bayesian solution is proposed to recover the dynamic noise variance and detect the occupancy of primary frequency band simultaneously. The states of primary users are detected based on particle filtering technology, and then, the noise parameters are tracked by using finite dimensional statistics for each particle based on marginalized adaptive particle filtering. Simulation results are provided to validate that the proposed method can improve the sensing performance significantly and target the dynamic noise variance accurately.**

***Index Terms*—Spectrum sensing, dynamic noise variance, marginalized adaptive particle filtering, joint estimation.**

I. Introduction

Cognitive radio (CR), as an effective technology to solve spectrum scarcity problem, was first proposed in [1]. CR has a potential to accomodate for the 5th generation (5G) communication system, since it can fully utilize all available non-contiguous spectrums flexibly and efficiently in 5G wireless networks [2]. However, the main challenge of CR is to circumvent inference to primary systems. One strategy for this challenge is that the secondary users (SUs) access to frequency bands opportunistically which are detected to be vacant. This flexible approach is defined as spectrum sensing (SS). It's important to note that the prior knowledge of noise distribution is crucial for SS. However, the SUs often need to detect primary signals accurately with imperfect knowledge of noise level which is referred to as noise uncertainty when implementing SS in the 5G communication system.

In order to deal with noise uncertainty, various SS methods are investigated [3]-[5]. Dong Chen et al. propose a combination method of cooperative SS with adaptive multiple thresholds in [3]. And according to [4], Chunyi Song et al. present a multi-antenna based SS method using the generalized likelihood ratio test (GLRT) paradigm to tackle noise uncertainty. These reports can address the noise uncertainty issue but are impractical to be applied to single-node single-antenna (SNSA) systems due to the high complexity of communication devices. In [5], Yonghong Zeng et al. present a SS algorithm based on the difference of statistical covariance matrix between transmitted signals and pure noise. This algorithm can be applied to SNSA systems, nevertheless, it requires high correlation of transmitted signals in space or time. In addition, the properties of noise process are often non-stationary due to the variability and uncertainty of wireless or mobile communication environment. But unfortunately, existing methods are designed for noise process with static statistical properties and the performance will deteriorate when being applied to CR systems with dynamic noise properties.

To overcome the challenge caused by non-stationary noise properties and also to alleviate the difficulty in future flexible deployments (e.g. D2D communications), we propose an effective SS method which can detect the PU states and track the noise variance jointly based on Bayesian inference framework. The proposed sensing algorithm is easy to be applied in SNSA systems with dynamic noise variance and doesn't require the correlation of transmitted signals. The main contributions of this correspondence can be summarized into two aspects.

Firstly, we formulate a dynamic state-space model (DSM) to depict SS system with dynamic noise variance. The PU states and noise variance are considered as hidden states and only the sampling observation of received signals is known to SU, hence the SS is converted into a blind estimation problem.

Secondly, based on the formulated DSM, a sequential estimation scheme is proposed which can monitor PU states and dynamic noise variance jointly and in real time at the receiver. This joint estimation framework is accomplished by utilizing marginalized adaptive particle filtering (MAPF) technology [6]. By tracking noise variance, the information uncertainty can be suppressed to the minimum, and the improvement of sensing performance will be achieved. Moreover, as an unexpected gift, the recovered noise variance will go far towards further CR enhancements especially in power allocation for spectrum sharing and is also helpful for SU to recognize the radio environment.

The rest of this correspondence is organized as follows. In Section II, we provide the DSM of SS system. The joint blind sensing algorithm is introduced in detail in Section III. In Section IV, numerical results and performance analysis are provided. And finally, conclusions are drawn in Section V.

The notations used in this correspondence are defined as follows. Symbols for vectors and matrices are in lowercase boldface and uppercase boldface respectively. $\lfloor\cdot\rfloor$ means the floor value. $\mathrm{E}(\cdot)$ denotes the ensemble average.

M. W. Sun, C. L. Zhao and Bin Li are with the School of Information Science and Engineering, Beijing University of Posts and Telecommunications, Beijing 100876, China (clzhao@bupt.edu.cn; stone_123456@126.com).

M. W. Sun is with the School of Engineering and Computing Sciences, Durham University, Durham DH1 3LE, UK (e-mail: mengwei.sun@durham.ac.uk).

Su Yan is with the State Radio Monitoring Center Testing Center, Beijing 100041, China. (e-mail: yansu@srtc.org.cn).

This work was supported by National Natural Science Foundation of China under Grants 61379016, Ph.D. Programs Foundation of the Education Ministry of China 20130005110016 and Foundation of China Scholarship Council.

II. System Model

We consider the following discrete time dynamic state-space model which relates the hidden PU state S_n and the noise variance σ_n^2 to the observation y_n.

$$[S_n, \mathbf{x}_n] = \Phi([S_{n-1}, \mathbf{x}_{n-1}]) \tag{1}$$

$$\sigma_n^2 = \Gamma(\sigma_{0:n-1}^2) \tag{2}$$

$$y_n = \Psi(\mathbf{x}_n, \mathbf{v}_n, \sigma_n^2) \tag{3}$$

Here, S_n in (1) denotes PU state and comes into two forms: active and dormant, and $\mathbf{x}_n$ represents the corresponding PU transmitted signal. The evolution behavior of S_n is characterized by TSMC [7] [8]. And the transition probability matrix (TPM) can be written as:

$$\mathbf{X} = \begin{bmatrix} p_{d\to d} & p_{d\to a} \\ p_{a\to d} & p_{a\to a} \end{bmatrix} = \begin{bmatrix} p_{00} & 1-p_{00} \\ 1-p_{11} & p_{11} \end{bmatrix} \tag{4}$$

In CR system, SU monitors PU states and transmits its own signal periodically, and this time frame structure is defined as sensing-transmission slot (STS) which comprises two parts, namely sensing time T_{s1} and signal transmission time T_{s2} respectively, and $T_{s1}+T_{s2} = T_s$ [9]. It should be noted that the PU state remains the same in one STS. In sensing time, the transmitted signals of PU $\mathbf{x}_n$ will be sampled and processed by SU. In this correspondence, M is set to denote the sampling size and n represents the STS index.

In (2), σ_n^2 is the actual noise variance at the n-th STS, and $\mathbf{v}_n = [v_{n,0}, v_{n,1}, \ldots, v_{n,M-1}]$ in (3) is an i.i.d sampling noise sequence where $v_{n,m} \sim N(0, \sigma_n^2)$. It's well-known that a stationary white Gaussian assumption of background noise is only an approximation as it ignores the distributional uncertainty [10]. Therefore, we assume that the receiver can narrow down the noise process within a set of distributions denoted by $\mathcal{W}_\varepsilon$, where ε represents the amount of average signal to noise ratio (SNR) uncertainty, i.e., there is at most ε dB uncertainty in $\mathcal{W}_\varepsilon$ [11]. Since the radiometer only sees energy, the distributional uncertainty of actual noise variance can be summarized in an interval $\sigma_n^2 \in \Sigma = [(1/\rho)\sigma_0^2, \rho\sigma_0^2]$ where $\rho = 10^{\frac{\varepsilon}{10}}$ and σ_0^2 represents the nominal noise variance which is associated with the uncertainty set $\mathcal{W}_\varepsilon$. In addition, the noise variance is assumed to be slow varying in this correspondence and a third order TS-AR process is utilized to model the dynamics of noise variance in view of autoregressive (AR) model can represent different types of random process and describe certain time-varying processes in signal processing [12]. Specifically, the state transform equation Γ in (2) is represented by:

$$\sigma_{n^\dagger}^2 = a_0\sigma_{n^\dagger-1}^2 + a_1\sigma_{n^\dagger-2}^2 + a_2\sigma_{n^\dagger-3}^2 + z_n^\dagger, \quad \sigma_{n^\dagger}^2 \in \Sigma \tag{5}$$

where $z_{n^\dagger}$ is white noise. $n^\dagger$ denotes noise variance time index, the relationship between $n^\dagger$ and STS index n is written as: $n^\dagger = \lfloor n/J \rfloor$, J is an integer greater than 1. Specifically, the evolution of noise variance is supposed to be slow varying and will be static over several STSs. Therefore, the STSs can be classified into two categories due to the different relationship with noise variance coherent period, i.e., first slot and non-first slot, and noise variance changes only in the first slots.

There are two hypotheses: H_0 denotes that the PU signal does not exist, while H_1 denotes that the PU signal exists. The observation under these two hypotheses are given by:

$$y_n = \begin{cases} \sum_{m=1}^{M} v_{n,m}, & H_0 \\ \sum_{m=1}^{M} (x_{n,m} + v_{n,m}), & H_1 \end{cases} \tag{6}$$

III. Spectrum Sensing Algorithm

The purpose of the proposed joint estimation algorithm is to detect hidden PU states $S_{0:n}$ together with unknown noise variance $\sigma_{0:n}^2$. We address this problem by concerning the joint posterior probability of transmitted signal and noise variance, i.e. $p(\sigma_n^2, \mathbf{x}_{0:n}|y_{0:n})$. From Bayesian perspective, the joint estimation could be achieved by maximum a posteriori probability (MAP) criterion.

$$(\widehat{\sigma}_{0:n}^2, \widehat{\mathbf{x}}_{0:n})^{\text{MAP}} = \arg\max \left[p(\sigma_{0:n}^2, \mathbf{x}_{0:n}|y_{0:n})\right] \tag{7}$$

Following the concept of marginalized particle filtering (MPF) [6], we decompose the joint posterior probability in (7) into conditional densities as follows:

$$p(\sigma_{0:n}^2, \mathbf{x}_{0:n}|y_{0:n}) = p(\sigma_{0:n}^2|\mathbf{x}_{0:n}, y_{0:n})p(\mathbf{x}_{0:n}|y_{0:n}) \tag{8}$$

We can conclude from (8) that the joint SS method consists of three steps: estimate PU transmitted signal using PF [13], track noise variance based on marginalization concept [14], and detect PU state by Neyman-Pearson (N-P) detector.

A. Estimation of PU Transmitted Signal

The posteriori distributions of transmitted signal $\mathbf{x}_n$ is approximated with discrete random measures based on PF [15], [16], and then, $\mathbf{x}_n$ is estimated by MAP criterion.

$$\widehat{\mathbf{x}}_n \approx \arg\max \left[\sum_{i=1}^{P} \omega_n^i \delta(\mathbf{x}_n - \mathbf{x}_n^i)\right] \tag{9}$$

Specifically, the particles are generated from an important distribution, i.e. $x_n^i \sim \pi(\mathbf{x}_n|\mathbf{x}_{0:n-1}^i, y_{0:n})$. And then, the important weights can be evaluated by [17]:

$$\widetilde{\omega}_n^i \propto \frac{p(\mathbf{x}_n^i, y_n|\mathbf{x}_{0:n-1}^i, y_{0:n-1})}{\pi(\mathbf{x}_n^i|\mathbf{x}_{0:n-1}^i)}\omega_{n-1}^i \tag{10}$$

where the marginal distribution $p(\mathbf{x}_n^i, y_n|\mathbf{x}_{0:n-1}^i, y_{0:n-1})$ can be computed by integrating out the unknown noise variance:

$$\begin{aligned} & p(\mathbf{x}_n^i, y_n|\mathbf{x}_{0:n-1}^i, y_{0:n-1}) \\ &= \int p(\mathbf{x}_n^i, y_n|\sigma_n^2, \mathbf{x}_{0:n-1}^i, y_{0:n-1})p(\sigma_n^2|\mathbf{x}_{0:n-1}^i, y_{0:n-1})d\sigma_n^2 \end{aligned} \tag{11}$$

The predictive distribution $p(\sigma_n^2|\mathbf{x}_{0:n-1}^i, y_{0:n-1})$ can be simplified as $p(\sigma_{n|n-1}^2)$ and we can rewrite (11) as:

$$\begin{aligned} & p(\mathbf{x}_n^i, y_n|\mathbf{x}_{0:n-1}^i, y_{0:n-1}) \\ &= \int p(\mathbf{x}_n^i, y_n|\sigma_n^2, \mathbf{x}_{0:n-1}^i, y_{0:n-1})p(\sigma_{n|n-1}^2)d\sigma_{n|n-1}^2 \\ &\propto \int p(y_n|\sigma_{n|n-1}^2, \mathbf{x}_{0:n}^i, y_{0:n-1})p(\mathbf{x}_n^i|\mathbf{x}_{0:n-1}^i)p(\sigma_{n|n-1}^2)d\sigma_{n|n-1}^2 \end{aligned} \tag{12}$$

Here, the prior probability of PU signal $p(\mathbf{x}_n^i|\mathbf{x}_{0:n-1}^i)$ is achieved by the TPM given in (4). And the likelihood function follows Gaussian distribution and can be obtained by:

This article has been accepted for publication in a future issue of this journal, but has not been fully edited. Content may change prior to final publication. Citation information: DOI 10.1109/TVT.2016.2596789, IEEE Transactions on Vehicular Technology

$$p(y_n|\sigma^2_{n|n-1}, \mathbf{x}^i_{0:n}, y_{0:n-1}) = \frac{1}{\sqrt{2\pi M\sigma^2_{n|n-1}}}\exp\left(-\frac{y_n - \sum_{m=1}^{M} x^i_{n,m}}{2M\sigma^2_{n|n-1}}\right) \tag{13}$$

Then, the important weights is normalized and the transmitted signal is derived with particles and associated importance weights based on asymptotical MAP criterion in (9).

B. Estimation of noise variance

It should be noted that the evolution of noise variance is characterized by slow varying, so it is difficult to get reliable and fixed estimation for the whole sensing process based on a refinement after several STSs. In order to overcome this problem, we designed an adaptive estimation mechanism which can track the evolution of noise variance in real time. More specifically, the estimated result of noise variance $\widehat{\sigma}^2_n$ equals to the statistical expectation of current posterior probability $p(\sigma^2_n|y_{0:n})$ depending on unbiased estimation. And $p(\sigma^2_n|y_{0:n})$ is approximated by the marginal posterior probability $p(\sigma^2_n|\mathbf{x}^i_{0:n}, y_{0:n})$ and the associated importance weights ω^i_n. Furthermore, the hyper-parameters of the marginal posterior probability are updated based on the the concept of conjugacy prior and the adaptive mechanism of forgetting factor designed in this correspondence. The concrete calculated steps for noise variance are shown as follows.

For noise following normal distribution with known mean and unknown variance, the conjugate prior is defined as an inverse Gamma (iG) distribution [14] and the hierarchical Bayesian model can be written as:

$$v_{n,m}|\sigma^2_n \sim N(0, \sigma^2_n) \tag{14}$$

$$\sigma^2_{n|n-1} \sim iG(\alpha^i_{n|n-1}, \beta^i_{n|n-1}) \propto \left(\frac{1}{\sigma^2_{n|n-1}}\right)^{\alpha^i_{n|n-1}+1} \exp\left(-\frac{\beta^i_{n|n-1}}{\sigma^2_{n|n-1}}\right) \tag{15}$$

where $\alpha^i_{n|n-1}$ and $\beta^i_{n|n-1}$ are the predictive hyper-parameters. Based on the derivation presented in (16), the posterior probability of noise variance also follows iG distribution.

And the hyper-parameters of the posterior distribution can be computed recursively as follows:

$$\alpha^i_{n|n} = \alpha^i_{n|n-1} + \frac{1}{2} \tag{17}$$

$$\beta^i_{n|n} = \beta^i_{n|n-1} + \frac{y_n - \sum_{m=1}^{M} x^i_{n,m}}{2M} \tag{18}$$

where the predictive hyper-parameters are updated as $\alpha^i_{n|n-1} = \lambda\alpha^i_{n-1|n-1}$ and $\beta^i_{n|n-1} = \lambda\beta^i_{n-1|n-1}$. Here, λ denotes forgetting factor which specifies how quickly the filter reduces the influence of past sample information. In this correspondence, we design an adaptive mechanism of forgetting factor. I.e., $\lambda = \lambda_1$ when STS is the first, and $\lambda = \lambda_2$ when it is the non-first, here, $\lambda_1 < \lambda_2 < 1$. Since the noise variance stays the same in non-first slots and more past sample information can be used to estimate the noise variance. This proposed mechanism can take advantage of the slow varying characteristic of noise variance and enhance estimation accuracy.

After $\alpha^i_{n|n}$ and $\beta^i_{n|n}$ are updated, the marginal posterior of σ^2_n can be computed relying on marginalization concept.

$$\begin{aligned} p(\sigma^2_n|y_{0:n}) &= \int p(\sigma^2_n|\mathbf{x}_{0:n}, y_{0:n})p(\mathbf{x}_{0:n}|y_{0:n})d\mathbf{x}_{0:n} \\ &\approx \sum_{i=1}^{P} p(\sigma^2_n|\mathbf{x}^i_{0:n}, y_{0:n})\omega^i_n \end{aligned} \tag{19}$$

Finally, depending on unbiased estimation, the estimated result of noise variance equals to the statistical expectation.

$$\widehat{\sigma}^2_n = \mathrm{E}(\sigma^2_n|y_{0:n}) = \sum_{i=1}^{P} \frac{\beta^i_{n|n}}{\alpha^i_{n|n} - 1}\omega^i_n, \quad \alpha^i_{n|n} > 1 \tag{20}$$

C. Detection of PU State

N-P decision policy is a simple threshold policy that only depends on the comparison of the observation at the current slot with the calculated threshold. Specifically, after the noise variance is estimated in real time, the threshold at the current slot ϑ_n can be calculated for a target probability of false alarm which is defined as $p_f = p(H_1|H_0)$.

$$\vartheta_n = \sqrt{2M}\widehat{\sigma}_n \mathrm{erf}^{-1}(1 - 2p_f) \tag{21}$$

The detection result of PU state $\widehat{S}_n$ can be achieved using N-P policy described as:

$$y_n \underset{H_1}{\overset{H_0}{\lesseqgtr}} \vartheta_n \tag{22}$$

And then, the detection probability p_d which is defined as $p_d = p(H_1|H_1)$ can be calculated.

IV. Simulation Results

The actual SNR is set as $SNR^{\dagger}$ and it can be calculated by:

$$SNR^{\dagger} = 10\log\frac{E_x}{E_{\sigma^2}} = 10\log\frac{\frac{1}{MN}\sum_{n=1}^{N}\sum_{m=1}^{M}|x_{m,n}|^2}{\frac{1}{N}\sum_{n=1}^{N}\sigma^2_n} \tag{23}$$

And the nominal SNR is denoted by SNR_0. As mentioned earlier, when the noise uncertainty exists in practice, the actual noise variance σ^2_n is distributed randomly around its nominal value σ^2_0 , i.e., $\sigma^2_n \in \Sigma = [(1/\rho)\sigma^2_0, \rho\sigma^2_0]$, $\rho > 1$. As far as the $SNR^{\dagger}$ is concerned in (23), it will be randomly ranged in $[SNR_0 - \varepsilon, SNR_0 + \varepsilon]$ dB. Here, $\varepsilon = 10\log\rho$.

In this section, we illustrate the sensing performance of the proposed SS method compared with covariance absolute value (CAV) detection algorithm proposed in [5] and traditional energy detection (ED) method with dynamic noise variance. And then, we evaluate the effects to estimation performance caused by different system parameters.

A. Comparison of sensing performance

1) The detection performance is firstly described through ROC curves in Fig.1, i.e., $p_d = p(H_1|H_1)$ versus $p_f = p(H_1|H_0)$. Here, $SNR^{\dagger}$ is set to be 0dB and $\varepsilon = 1$dB. It is obvious that the proposed algorithm can achieve higher detection probability under the same probability of false alarm. The specific causes may be grouped under two heads. Firstly, based on the accurate real-time estimation of noise variance,

This article has been accepted for publication in a future issue of this journal, but has not been fully edited. Content may change prior to final publication. Citation information: DOI 10.1109/TVT.2016.2596789, IEEE Transactions on Vehicular Technology

$$
\begin{aligned}
p(\sigma_n^2|\mathbf{x}_{0:n}^i, y_{0:n}) &= \frac{p(y_n|\sigma_n^2, \mathbf{x}_{0:n}^i, y_{0:n-1})p(\mathbf{x}_n^i|\sigma_n^2, \mathbf{x}_{0:n-1}^i, y_{0:n-1})p(\sigma_n^2|\mathbf{x}_{0:n-1}^i, y_{0:n-1})}{p(y_n|\mathbf{x}_{0:n}^i, y_{0:n-1})p(\mathbf{x}_n^i|\mathbf{x}_{0:n-1}^i, y_{0:n-1})} = \frac{p(y_n|\sigma_n^2, \mathbf{x}_{0:n}^i, y_{0:n-1})p(\sigma_n^2|\mathbf{x}_{0:n-1}^i, y_{0:n-1})}{\int p(y_n|\sigma_n^2, \mathbf{x}_{0:n}^i, y_{0:n-1})p(\sigma_n^2|\mathbf{x}_{0:n-1}^i, y_{0:n-1})d\sigma_n^2} \\
&\propto p(y_n|\sigma_n^2, \mathbf{x}_{0:n}^i, y_{0:n-1})p(\sigma_{n|n-1}^2) \propto \frac{1}{\sqrt{2\pi M\sigma_n^2}}\exp\left(-\frac{y_n - \sum_{m=1}^M x_{n,m}^i}{2M\sigma_n^2}\right) \times \left(\frac{1}{\sigma_n^2}\right)^{\alpha_{n|n-1}^i+1} \exp\left(-\frac{\beta_{n|n-1}^i}{\sigma_n^2}\right) \\
&\propto \left(\frac{1}{\sigma_n^2}\right)^{\left(\alpha_{n|n-1}^i+\frac{1}{2}\right)+1} \exp\left[-\frac{\beta_{n|n-1}^i + \left(y_n - \sum_{m=1}^M x_{n,m}^i\right)/(2M)}{\sigma_n^2}\right]
\end{aligned} \tag{16}
$$

an accurate real-time threshold can be obtained which can be used for N-P decision policy. By contrast, the threshold for ED method is obtained relying on the nominal noise variance σ_0^2 and it can't be accurate. Secondly, CAV method can suppress the information uncertainty when there is high correlation of transmitted signals in space or time. The correlation of transmitted signals set in this correspondence does exist but is not high enough, so the sensing performance of CAV method is beyond ED method but still behind the proposed method.

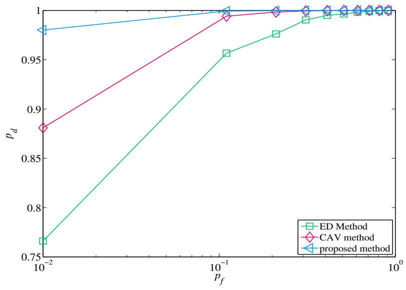

Fig. 1. ROC curves of the proposed algorithm compared with CAV and ED

2) Next, we set the target $p_f = 0.1$, and the detection probabilities p_d of different uncertainty parameters ε under increasing $SNR^{\dagger}$ are compared in Fig.2 (The corresponding actual average value of p_f is shown in Table I). Here, $\varepsilon = 0, 1,$ and 5dB due to the parameter setup in [5] and [10]. And the x-axis in Fig.2 denotes the true value of SNR, i.e, $SNR^{\dagger}$.

TABLE I
PROBABILITIES OF FALSE ALARM

method \ ε	0dB	1dB	5dB
ED	0.1090	0.1117	0.1266
CAV	0.1000	0.1001	0.1001
proposed method	0.0928	0.0927	0.0939

From Table I and Fig.2, we can see that p_f of ED exceeds the target false alarm probability and p_d of ED is lower than other methods and very sensitive to noise uncertainty while p_f and p_d of the CAV and proposed methods are not very sensitive to noise uncertainty. Since the information uncertainty of noise can be suppressed to the minimum by tracking the noise variance accurately with the proposed algorithm. And the validity of the CAV algorithm only relies on the assumption that the signal samples are correlated.

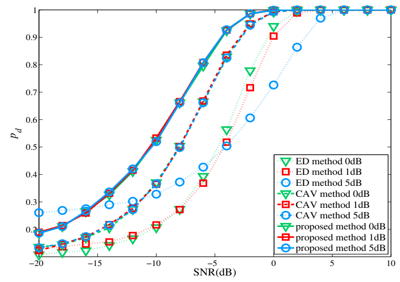

Fig. 2. Detection performance comparison under different noise uncertainty

B. Estimation performance with different parameters

1) In this section, we firstly evaluate the effects of changing forgetting factors to the estimation performance of noise variance as shown in Fig.3. The estimation results are provided for two realizations, i.e., realization1 $\{\lambda_1 = 0.98, \lambda_2 = 0.985\}$ and realization2 $\{\lambda_1 = 0.96, \lambda_2 = 0.965\}$. One can observe from the results that the fluctuation of estimation are more turbulent for smaller λ but can track changes of the noise variance more rapidly. On the other hand, smoother estimation can be obtained by larger λ, however, it will lead to a slower response to changes. The reason is that larger forgetting factor means that the information of current observation accounts for a lower proportion of the whole utilized information, so it is more difficult to track changes rapidly.

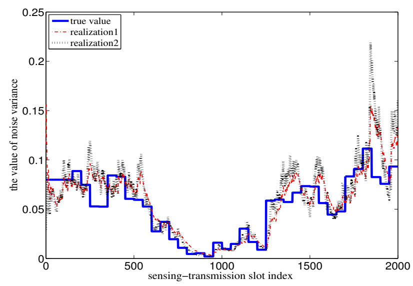

Fig. 3. Estimated noise variance for different forgetting factors λ

2) And the mean-square error (MSE) performance of estimated noise variance under different forgetting factors λ is shown in Fig.4. Five sets of forgetting factors are considered, i.e., realization1 $\{\lambda_1 = 0.94, \lambda_2 = 0.945\}$, realization2 $\{\lambda_1 = 0.96, \lambda_2 = 0.965\}$, realization3 $\{\lambda_1 = 0.98, \lambda_2 = 0.985\}$, realization4 $\{\lambda_1 = 0.99, \lambda_2 = 0.995\}$ and realization5 $\{\lambda_1 = 1,$

This article has been accepted for publication in a future issue of this journal, but has not been fully edited. Content may change prior to final publication. Citation information: DOI 10.1109/TVT.2016.2596789, IEEE Transactions on Vehicular Technology

$\lambda_2 = 1\}$. It is seen that along with the increase of forgetting factors, the MSE of realization3 is less than realization1 and realization2. This is because the fluctuation of actual noise variance set in this investigation is not sharp, the fluctuation of estimation caused by smaller forgetting factors will increase the estimation error. However, when the forgetting factors are large enough such as the sets of realization4 and realization5, the estimation performance will become less satisfactory since it can't track the changes of noise variance.

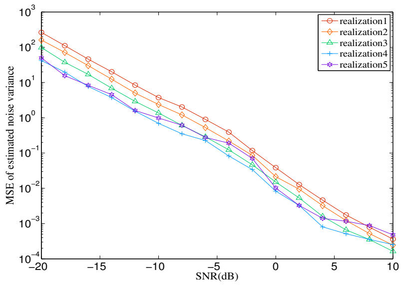

Fig. 4. Estimation performance of noise variance under different λ

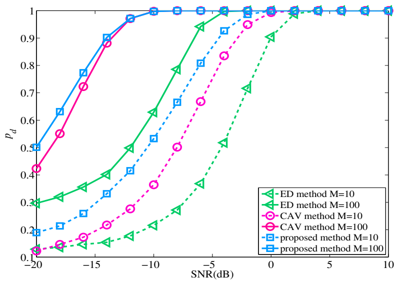

Fig. 5. Sensing performance of the proposed algorithm under different M

3) Then, we study the effects on detection performance caused by different sampling size M. And two typical configurations of M are considered, i.e., $M = 10$ and 100 [7], [18]. It is observed from Fig.5 that increasing sampling size is an effective way to enhance detection performance of all detection methods. In addition, compared with ED method, the superior detection performance of the proposed algorithm still maintaines even though the sampling size increases.

C. Analysis of Computational Complexity

The CAV method requires about M^2 multiplications when computing the autocorrelations of received signal, which is why its complexity is about $O(M^2)$ [5]. In contrast, ED method has a lower complexity than $O(M)$, since the decision threshold can be implemented using a lookup table for $Q_{\chi^2}^{-1}(\cdot)$ function and be reused [19]. While the proposed detection algorithm is independent of sampling size M and, therefore, we could measure it by $O(E)$ which is related to particle size P. To sum up, the complexity of the proposed algorithm and ED method can be regarded as the same order of magnitude and much smaller than CAV when the sampling size M is large enough.

V. Conclusions

In this correspondence, we develop a novel SS algorithm for CR systems with dynamic noise variance. By fully exploiting the dynamic properties of PU state and noise variance, a DSM is formulated and a sequential spectrum scheme is designed by tracking the dynamic noise variance and PU states jointly. Simulation results have been provided to validate the satisfactory sensing performance of the proposed algorithm.

References

[1] Federal Communication Commission, Spectrum Policy Task Force Report, ET Docket no. 02-155, Nov. 2002.
[2] Huawei, 5G: A Technology Vision, Huawei Europe, Jan. 2014.
[3] D. Chen, J. Li, and J. Ma, "Cooperative spectrum sensing under noise uncertainty in cognitive radio," in *Proc. Wireless Communications, Networking and Mobile Computing*, Dalian, China, Oct. 2008, pp. 1-4.
[4] C. Song, Y. D. Alemseged, H. N. Tran, et al, "Adaptive two thresholds based energy detection for cooperative spectrum sensing," in *Proc. Consumer Communications and Networking*, Las Vegas, USA, Jan. 2010, pp. 1-6.
[5] Y. Zeng, and Y. C. Liang, "Spectrum-sensing algorithms for cognitive radio based on statistical covariances," *IEEE Trans. Veh. Technol.*, vol. 58, no. 4, pp. 1804-1815, May. 2009.
[6] E. Ozkana, V. Smidlb, S. Sahaa, et al, "Marginalized adaptive particle filtering for nonlinear models with unknown time-varying noise parameters," *Automatica*, vol. 49, no. 6, pp. 1566-1575, Jun. 2013.
[7] B. Li, C. L. Zhao, M. W. Sun, et al, "Spectrum sensing for cognitive radios in time-variant flat fading channels: A joint estimation approach," *IEEE Trans. Commun.*, vol. 62, no. 8, pp. 2665-2680, Aug. 2014.
[8] B. Li, J. Hou, X. Li, et al, "Deep Sensing for Space-Time Doubly Selective Channels: When a Primary User is Mobile and the Channel is Flat Rayleigh Fading," *IEEE Trans. Signal Process.*, vol. 64, no. 13, pp. 3362-3375, Jan 2016.
[9] M. W. Sun, S. H. Li, B. Li, et al,"Spectrum Sensing for Self-Organizing Network in the Presence of Time-Variant Multipath Flat Fading Channels and Unknown Noise Variance," *Mobile Netw Appl.*, vol. 20, no. 4, pp. 435-448, Aug. 2015.
[10] R. Tandra and A. Sahai, "SNR Walls for Signal Detection," *IEEE J. Sel. Topics Signal Process*, vol. 2, no. 1, pp. 4-17, Feb. 2008.
[11] R. Tandra and A. Sahai, "Fundamental limits on detection in low SNR under noise uncertainty," in *Proc. 2005 International Conference on Wireless Networks, Communications and Mobile Computing*, Maui, HI, Jun. 2005, pp. 464-469.
[12] L. Jackson, J. Huang, and K. Richards, "AR, ARMA, and AR-in-noise modeling by fitting windowed correlation data," in *Proc. Acoustics, Speech, and Signal Processing, IEEE International Conference on ICASSP*, Texas, USA, Apr. 1987, pp. 2039-2042.
[13] B. Li, S. H. Li, A. Nallanathan, et al, "Deep Sensing for Future Spectrum and Location Awareness 5G Communications," *IEEE J. Sel. Areas Commun.*, vol. 33, no. 7, pp.1331-1344, July. 2015.
[14] S. Saha, E. Ozkan, F. Gustafsson, et al, "Marginalized particle filters for Bayesian estimation of Gaussian noise parameters," in *Proc. 13th Conference on Information Fusion (FUSION)*, Edinburgh, UK, Jul. 2010, pp. 1-8.
[15] B. Li, M. W. Sun, X. F. Li, et al, "Energy Detection Based Spectrum Sensing for Cognitive Radios Over Time-Frequency Doubly Selective Fading Channels," *IEEE Signal Process.*, vol. 63, no. 2, pp. 402-417, Jan. 2015.
[16] M. W. Sun, B. Li, Q. Z. Song, et al, "Joint detection scheme for spectrum sensing over time-variant flat fading channels," *IET Commun.*, vol. 8, no. 12, pp. 2064-2073, Aug. 2014.
[17] J. Miguez and P. M. Djuric, "Blind equalization by sequential importance sampling," in *Proc. IEEE International Symposium on Circuits and Systems (ISCAS)*, Arizona, Scottsdale, May. 2002, pp. I-845-I-848.
[18] B. Li, S. H. Li, A. Nallanathan, et al, "Deep Sensing for Next-Generation Dynamic Spectrum Sharing: More Than Detecting the Occupancy State of Primary Spectrum," *IEEE Trans. Commun.*, vol. 63, no. 7, pp. 2442-2457, Jul. 2015.
[19] W. L. Chin, J. M. Li, and H. H. Chen, "Low-Complexity Energy Detection for Spectrum Sensing With Random Arrivals of Primary Users," *IEEE Tran. Veh Technol.*, vol. 65, no. 2, pp. 947-952, Feb. 2016.